NUMERICAL CALCULATION OF SMALL-ANGLE COLLIMATOR WAKEFIELDS FOR SHORT BUNCHES

I. Zagorodnov, T. Weiland

TEMF, Fachbereich 18, TU Darmstadt, 64287 Darmstadt, Germany

K.L.F. Bane

SLAC, Stanford University, Stanford, CA 94309, USA

Abstract

Collimators are used to eliminate halo particles from the beam. To relax the wakefield effects a gradual transition from a large to a small aperture is used. However, the existing computer codes face severe problems for long tapered transitions. Two main sources of the problems are the grid dispersion and the staircase geometry approximation. Using recently developed time domain numerical approach, which is able to model curved boundaries and does not suffer from dispersion in longitudinal direction, we calculate the short-range geometric wakefields of the TESLA and NLC collimators. Wake fields and corresponding integral parameters are given for bunches of different length. The numerical results are compared to measurements and to analytical estimations. The applicability range for the analytical formulas is highlighted.

1 INTRODUCTION

The short-range wakefields of the collimators are of a special concern for future colliders with extremely small transverse emmitance of the beam. The longitudinal wakes increase the energy spread and the transverse wakes spoil projected emmitance of the beam.

The wakefield effects can be decreased by tapering the steps with small angles. To perform the optimization, one has to compute wakes numerically or analytically. Conventional codes face problems for smoothly tapered long transition. Using recently developed time domain numerical approach [1], which is able to model curved boundaries and does not suffer from dispersion in longitudinal direction, we calculate with high accuracy the short-range longitudinal and transverse wakefields of the TESLA and NLC collimators.

The numerical results are compared to measurements and to analytical estimations. The applicability range of analytical formulas is highlighted. Optimization of TESLA TTF2 collimator's geometry is considered.

2 ANALYTICAL ESTIMATIONS

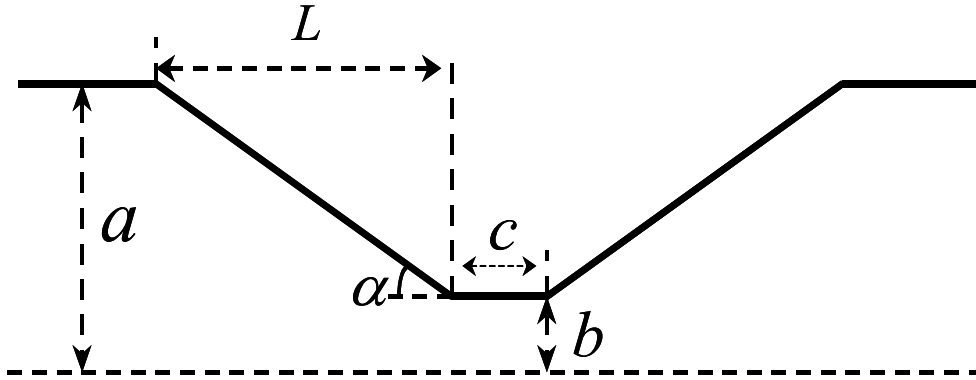This paper deals with circular collimator whose geometry is outlined in the Fig.1.

Fig.1. Geometry of the collimator

As shown in [2], for small taper angles $\rho = \tan(\alpha)b/\sigma \ll 1$ (σ is a width of Gaussian bunch) the collimator is in the *inductive* regime and the impedance estimations read

$$Z_{\parallel}^{0} = \Theta \frac{i\omega}{c^2} \int_{-\infty}^{\infty} \left(f'\right)^2 dz, \tag{1}$$

$$Z_{\perp}^{1} = \Theta \frac{2i}{c} \int_{-\infty}^{\infty} \left(\frac{f'}{f}\right)^2 dz, \tag{2}$$

where $f(z)$ is the pipe radius, $\Theta = Z_0 c/4\pi$, and Z_0 is the free space impedance.

3 NUMERICAL METHOD

Consider a perfectly conducting structure S and assume that the bunch is moving in domain Ω with the velocity of light $\mathbf{c}$ and is characterized by a charge distribution ρ. The bunch introduces an electric current $\mathbf{j} = \mathbf{c}\rho$ and the following system has to be solved

$$\nabla \times \mathbf{H} = \frac{\partial}{\partial t}\mathbf{D} + \mathbf{j}, \nabla \times \mathbf{E} = -\frac{\partial}{\partial t}\mathbf{B}, \tag{3}$$

$$\nabla \cdot \mathbf{D} = \rho, \nabla \cdot \mathbf{B} = 0$$

$$\mathbf{H} = \mu^{-1}\mathbf{B}, \mathbf{D} = \varepsilon\mathbf{E}, x \in \Omega, \quad \mathbf{n} \times \mathbf{E} = 0, \quad x \in S$$

The full field $\mathbf{D}, \mathbf{H}$ can be decomposed into the field of the bunch in free space $\mathbf{D}^0, \mathbf{H}^0$ and a scattered field

$$\mathbf{D}^s = \mathbf{D} - \mathbf{D}^0, \quad \mathbf{H}^s = \mathbf{H} - \mathbf{H}^0. \tag{4}$$

The scattered field can be presented by vector potential $\mathbf{A}$:

$$\mathbf{D}^s = \nabla \times \mathbf{A}, \quad \mathbf{H}^s = \frac{\partial}{\partial t}\mathbf{A}. \tag{5}$$

Substitution of formulas (5) into system (3) leads to the problem for the vector potential $\mathbf{A}$

$$\nabla \times \nabla \times \mathbf{A} = -\frac{\partial^2}{c^2 \partial t^2}\mathbf{A}, \quad \nabla \cdot \mathbf{A} = 0, \quad x \in \Omega, \tag{6}$$

$$\mathbf{n} \cdot \mathbf{A} = -\int_{-\infty}^{t} \mathbf{n} \cdot \mathbf{H}^0 d\tau, \quad \mathbf{n} \times \nabla \times \mathbf{A} = -\int_{-\infty}^{t} \mathbf{n} \times \nabla \times \mathbf{H}^0 d\tau, \quad x \in S.$$

A numerical scheme for the vector potential $\mathbf{A}$ reads [1]:

$$(\mathbf{I} + \theta\mathbf{T})\mathbf{a}^{n+1} = 2\mathbf{a}^n - \mathbf{a}^{n-1} - \mathbf{T}((1-2\theta)\mathbf{a}^n + \theta\mathbf{a}^{n-1}) - \mathbf{L}\mathbf{a}^n + \mathbf{F}^n, \tag{7}$$

$$\mathbf{T} = \Delta t^2 \mathbf{M}_{\mu^{-1}}\mathbf{C}\mathbf{M}_{\varepsilon^{-1}}\mathbf{C}_1^T, \quad \mathbf{L} = \Delta t^2 \mathbf{M}_{\mu^{-1}}\mathbf{C}\mathbf{M}_{\varepsilon^{-1}}\mathbf{C}_2^T,$$

$$\mathbf{F}^n = -(\mathbf{I} + \theta\mathbf{T})\mathbf{a}_0^{n+1} + 2\mathbf{a}_0^n - \mathbf{a}_0^{n-1} - \mathbf{T}((1-2\theta)\mathbf{a}_0^n + \theta\mathbf{a}_0^{n-1}) - \mathbf{L}\mathbf{a}_0^n,$$

$$\mathbf{a}^n = \int_{-\infty}^{t_n} \widehat{\mathbf{h}}_s d\tau, \quad \mathbf{a}_0^n = \int_{-\infty}^{t_n} \widehat{\mathbf{h}}_0 d\tau,$$

where vectors $\widehat{\mathbf{h}}_0$, $\widehat{\mathbf{h}}_s$ correspond to the fields $\mathbf{H}^0$, $\mathbf{H}^s$ in representation (4). Scheme (7) approximates problem (6). $\mathbf{F}^n$ approximates the boundary conditions. Above we have split the discrete curl operator [3] $\tilde{\mathbf{C}} = \mathbf{C}^T$ into the transversal operator $\mathbf{C}_1^T$ and the longitudinal operator $\mathbf{C}_2^T$ and θ is a numerical parameter to be defined. If we note the longitudinal coordinate by z and the transversal coordinates by r, φ, the operators have the form

$$\mathbf{C}_1^T = \begin{pmatrix} 0 & 0 & -\mathbf{P}_\varphi^T \\ 0 & 0 & \mathbf{P}_r^T \\ \mathbf{P}_\varphi^T & -\mathbf{P}_r^T & 0 \end{pmatrix}, \quad \mathbf{C}_2^T = \begin{pmatrix} 0 & \mathbf{P}_z^T & 0 \\ -\mathbf{P}_z^T & 0 & 0 \\ 0 & 0 & 0 \end{pmatrix}.$$

With the time step $c\Delta t = \Delta z$ allowed by stability condition, the scheme has no dispersion in the longitudinal direction and a moving mesh can be employed easily.

To reduce dispersion in the transversal direction minimal allowed value of $\theta = 0.25$ is used. To overcome the staircase problem, the approach invented in [4] is adopted.

In the case of circular structure, the algorithm requires the same order of operations as the explicit FDTD method and for longitudinal case (monopole mode) and staircase geometry approximation our scheme with $\theta = 0.5$ is reduced to the one presented in [5].

4 NUMERICAL RESULTS

The new numerical scheme is implemented in the code ECHO.

In the first example we consider a circular collimator with parameters typical to TESLA project: $a = 17.5mm$, $b = 0.4mm$, $c = 20mm$, and Gaussian bunch with $\sigma = 0.3mm$.

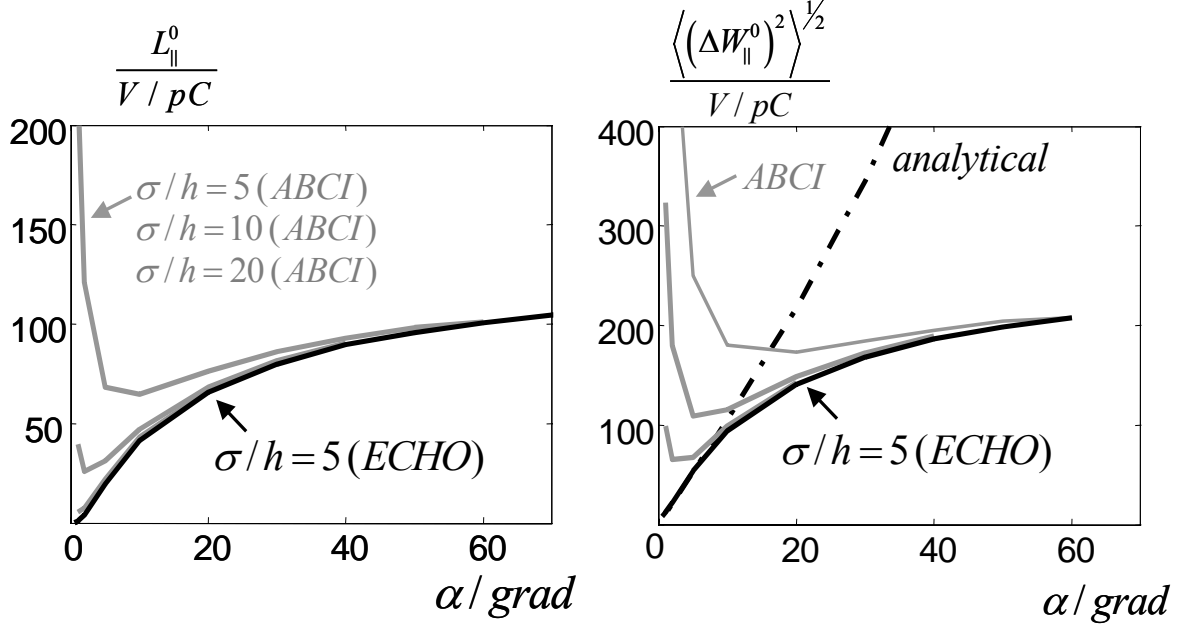Fig 2. Longitudinal wake dependence
on the collimator angle

Fig. 2 shows dependence of the longitudinal loss factor (left)

$$L_\parallel^0 = \left\langle W_\parallel^0 \right\rangle = \frac{1}{Q} \int_{-\infty}^{\infty} W_\parallel^0(s)q(s)ds$$

and energy spread (right)

$$\left\langle \left(\Delta W_\parallel^0\right)^2 \right\rangle^{1/2} = \left[\frac{1}{Q} \int_{-\infty}^{\infty} \left(\left\langle W_\parallel^0 \right\rangle - W_\parallel^0(s)\right)^2 q(s)ds \right]^{1/2}$$

versus the angle α of the collimator. The black solid lines show the results obtained by the new code ECHO, the gray solid lines show the results from ABCI code [6], and the dashed line on the right picture shows analytical estimation obtained from the Yokoya's formula (1). The impedance (1) is inductive and the corresponding analytical loss factor is equal to zero. The wakes were calculated up to the angle $\alpha = 0.5^o$ that corresponds to the total collimator length $\sim 4m$. As it is seen the code ABCI shows wrong behavior of the curves for limit $\alpha \to 0$. The ECHO curves follow analytical estimation (1) for small-angle collimators. On the right picture at $\alpha = 10^o$ ($\rho = \tan(\alpha)b/\sigma = 0.24$) the difference between analytical and numerical estimations is about 10% and at $\alpha = 5^o$ it is below 3%.

Fig. 3 shows the dependence of the dipole kick factor (left) and kick spread (right) on the angle α of the collimator. The solid lines show the results obtained by the code ECHO and the dashed lines show analytical estimations obtained from the Yokoya's formula (2) in Mathematica. The wakes were calculated up to the angle $\alpha = 0.5^{o}$. For small angles the ECHO curves follow the analytical estimation (2). On the right hand side picture at $\alpha = 20^{o}$ ($\rho = 0.5$) the difference between analytical and numerical estimations is about 7%.

Note that accuracy of the numerical results at given above test points $\alpha = 5^{o}, 10^{o}, 20^{o}$ is better than 1%. It was checked by recalculating the results for two and four times denser meshes.
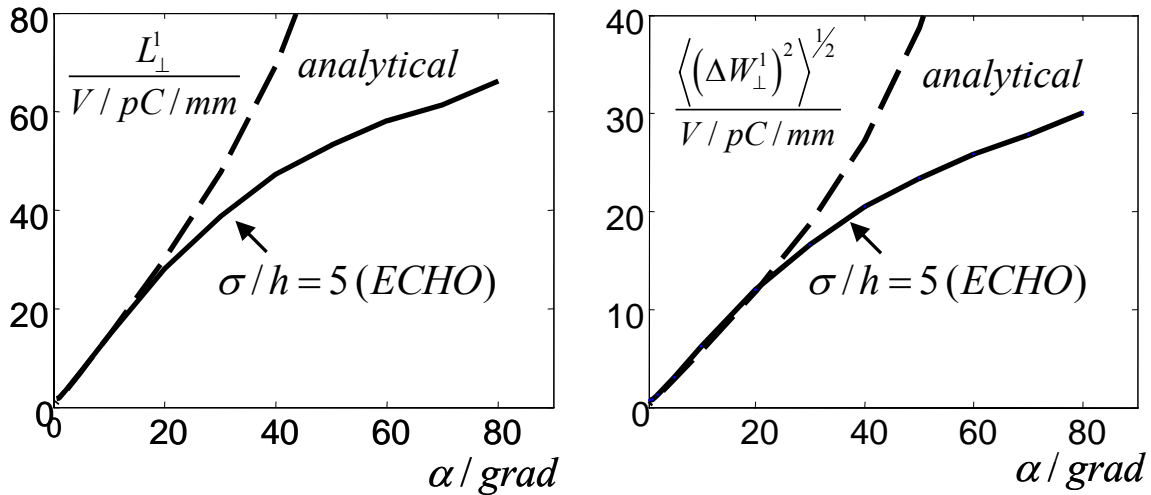

Fig 3. Transverse wake dependence on the collimator angle

The *absolute* error for the new code ECHO remains approximately on the same level regardless of the length of the collimator. ABCI requires a much more dense mesh for the same accuracy, strongly depending on the collimator length.

However, the *relative* error in the ECHO calculation increases for small angles since the sought wake fields aim at zero.
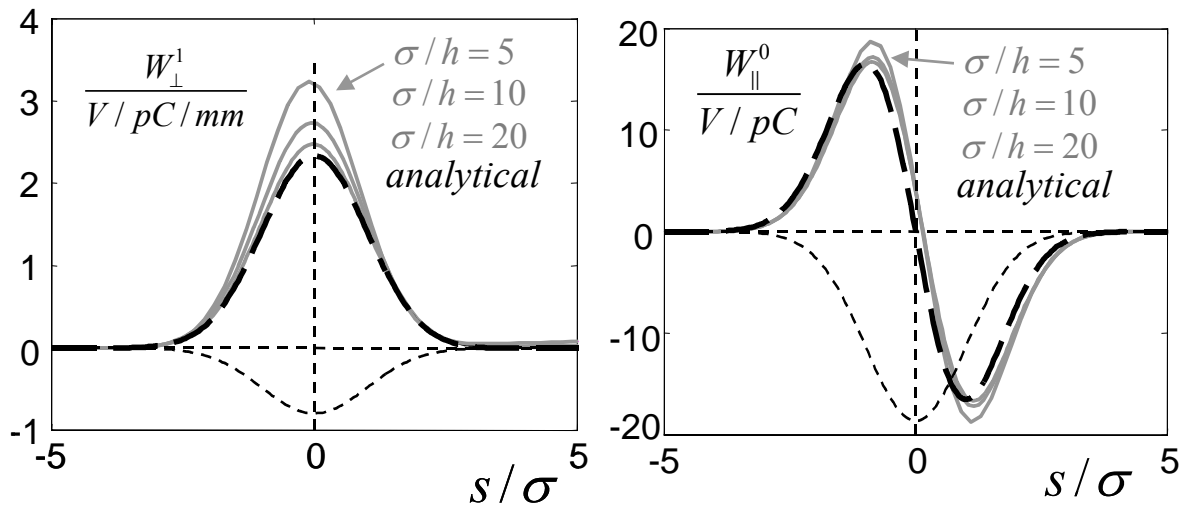

Fig 4. Wakes of the small angle collimator

Fig.4. shows longitudinal (left) and transversal (right) wake potentials for the small-angle collimator with angle $\alpha = 20mrad$. Dashed lines show analytical estimations (1), (2), and solid gray lines show the results from ECHO calculations. Numerical values of loss and kick factors are given at the Table 1.

σ/h	Loss, V/pC		Kick, V/pC/mm	
	TESLA	NLC	TESLA	NLC
5	1.46	33.6	2.24 (135)	12.8
10	1.42	**32.9**	1.91 (44.3)	11.2
20	**1.42**	-	1.74 (13.4)	10.6
Analytical	0		**1.65**	**10**

Table 1. Wake parameters of the collimators

Estimated values for kick parameters for the set of NLC parameters: $a = 17.5mm$, $b = 0.2mm$, $c = 20mm$, $\alpha = 20mrad$, $L = 865mm$ and Gaussian bunch with $\sigma = 0.1mm$. The kick factor calculated by ABCI I is given in parenthesis.
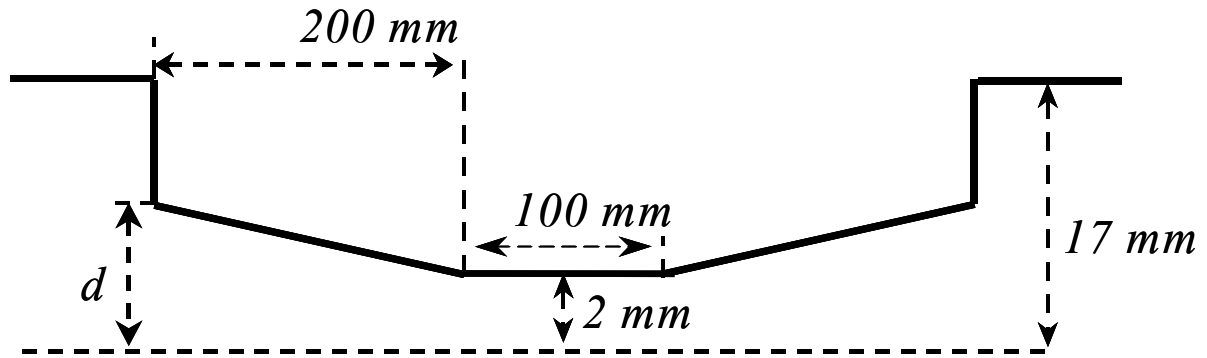

Fig 5. Geometry of the "step+taper" collimator

As it is seen from the above calculations, the tapering actually reduces considerably the wakes of the collimator. However, in order to obtain significant effect the collimator has to be too long. As alternative solution we consider "step+taper" geometry of the collimator shown in Fig.5. The effectiveness of such kind of geometry was proved in [7]. The set of parameters shown in Fig. 5 corresponds to TESLA TTF2 collimator at DESY [8]. The calculations are carried out for very short Gaussian bunch with $\sigma = 0.05mm$.
Fig. 6 shows dependence of the loss factor, energy spread (left) and kick factor, kick spread (right) on the parameter d (see Fig.5). As we see all functions have minimums and the value $d = 4.5mm$ can be taken as the optimum.

Finally, we compare our numerical results with experimental data. In order to obtain experimental data a dedicated beam test chamber was constructed and installed at the 1.19 GeV point in the SLAC linac [9]. The real collimator has square aperture. In our calculation it was approximated by circular collimator with the set of parameters: $a = 19mm$, $b = 1.9mm$, $c = 0mm$, $\alpha = 335mrad$, $L = 51mm$.

The measured data are given in the Table 2. The numerical results are simulated by ECHO and their accuracy is better than 1% (checked by thickening of the mesh). Analytical

results outside of parenthesis are calculated in Mathematica and correspond to Yokoya's formula (2).
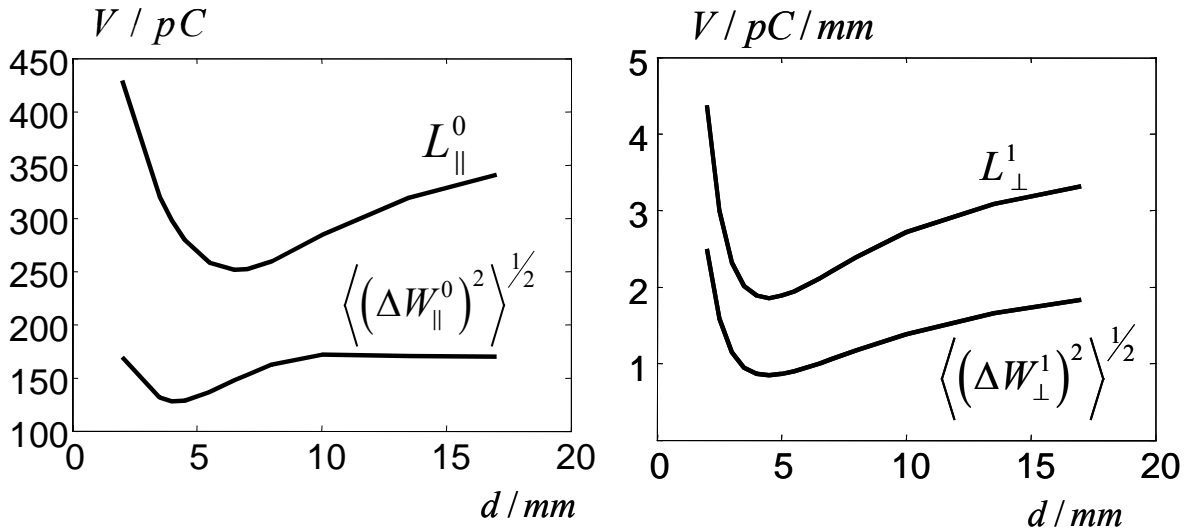

Fig 6. Collimator geometry optimization

The measured, simulated and analytically estimated results show good agreement for the Gaussian bunch with $\sigma = 1.2mm$. The factor $\rho = \tan(\alpha)b/\sigma$ is equal to 0.55 and the collimator is in inductive regime.

σ, mm	Kick factors, V/pC/mm		
	Measured	Simulated	Analytical
1.2	1.2 ± 0.1	1.268	1.34
0.65	1.4 ± 0.1	1.908	2.48

Table 2. Comparison of the measured, simulated
and analytical kick factors.

For the bunch with $\sigma = 0.65mm$ the data show disagreement. The factor $\rho = \tan(\alpha)b/\sigma$ is equal to 1.02 and inductive regime formula (1) is not applicable. The disagreement between simulated and measured data for bunch with $\sigma = 0.65mm$ is not understood and demands further investigations.

CONCLUSION

A new recently developed time domain numerical approach, which is able to model curved boundaries and does not suffer from dispersion in longitudinal direction is presented.
The short-range geometric wakefields of the TESLA and NLC collimators are calculated for bunches of different length. The numerical results are confirmed by comparison to analytical estimations.

ACKNOWLEGDEMENT

REFERENCES

[1] Zagorodnov, I., Weiland, T., *Calculation of Transversal Wake Potential for Short Bunches* // Proc. of ICAP 2002 (to appear).

[2] Yokoya, K., *Impedance of Slowly Tapered Structures*, Tech. Rep. SL/90-88 (AP), CERN, 1990.

[3] Weiland, T., *Time Domain Electromagnetic Field Computation with Finite Difference Methods*, Int. J. Numer. Model., Vol. 9, 1996, pp. 295-319.

[4] Zagorodnov, I., Schuhmann, R., Weiland, T., *A Uniformly Stable Conformal FDTD-Method on Cartesian Grids,* Int. J. Numer. Model., Vol. 16, 2003.

[5] Novokhatski, A., Timm, M., Weiland, T., *Transition Dynamics of the Wake Fields of Ultra Short Bunches*, ICAP 1998, Monterey, California, 1998.

[6] Chin, Y.H., *User's Guide for ABCI Version 8.7*, CERN-SL-94-02-AP.

[7] Bane, K.F.L., Morton, P.L., *Deflection by the Image Current and Charges of a Beam Scraper*, LINAC 1986, SLAC-PUB-3983

[8] Körfer, M., *Layout and Functionality of Collimator System*, TESLA Coll. Meeting, Salzau, 21.01.2003.

[9] Tenenbaum, P. et al., *Transverse Wakefields from Tapered Collimators: Measurement and Analysis*, PAC 2001, SLAC-PUB-8937.